Clinical Oral Investigations (2020) 24:3093–3103
https://doi.org/10.1007/s00784-019-03181-8

ORIGINAL ARTICLE

Effects of additional collagen in biphasic calcium phosphates: a study in a rabbit calvaria

Benoit Schaller[1] · Masako Fujioka-Kobayashi[1] · Claudio Zihlmann[2] · Viola Christina Schuler[1] · Hiroki Katagiri[1,3] · Niklaus P. Lang[1] · Nikola Saulacic[1]

Received: 29 August 2019 / Accepted: 19 December 2019 / Published online: 17 January 2020

Abstract

Objectives Biphasic calcium phosphates (BCP) are synthetic biomaterials developed as an alternative to the autogenous bone grafts and xenografts. The aim of the present study was to assess the influence of the addition of collagen onto the BCP resorption rate and bone formation.

Material and methods Eighteen male NWZ rabbits approximately 12 weeks of age were used. Critical size defects were randomly treated with bilayered BCP materials comprising 12% HA and 88% α-TCP with and without collagen or sham-operated, respectively. All defects were covered with a resorbable collagen membrane. Animals were euthanized after 3 and 12 weeks of healing and investigated by micro-CT, histologic, and histomorphometric analysis.

Results Woven bone formation was observed from the original bone at 3-week healing in all samples. After 3 months, mainly lamellar new bone in the peripheral area was observed. In the central region, both woven and lamellar bone were seen. Samples containing collagen showed less residual biomaterial than without collagen at both healing periods. Both types of granules were in close contact with new bone, yielding a complete defect closure at 3 months of healing. However, new bone volume and area was similar for both biomaterials.

Conclusions Within its limitations, the study results qualify collagen as a biocompatible carrier for BCPs. The presence of collagen indicated neither significant impact on the resorption of the BCPs nor on bone formation.

Clinical relevance The addition of collagen to BCPs might not be beneficial for the augmentation of extended bone deficiencies.

Keywords Animal experiments · Biomaterials · Bone substitutes · Guided tissue regeneration · Bone regeneration · Morphometric analysis

Introduction

Autogenous bone grafts, allografts, xenografts, as well as synthetic/alloplastic bone substitutes have been used in the treatment of atrophic jaw bone. Autogenous bone grafts predictably show osteoconductivity and possibly osteoinductivity [1]. However, possible donor site morbidity following the autogenous bone harvesting is a major issue [2]. Extensive research has been undertaken in the last decades to develop an appropriate bone substitute material. Clinically, bone substitutes in a granulated form applied under the principle of guided bone regeneration resulted in highly predictable treatment outcomes [3].

An ideal bone substitute should be remodeled and replaced by bone as a similar absorption rate as that encountered during bone formation [4]. However, healing times of defects treated with bone substitutes may be prolonged when compared to the particulated autogenous bone grafts. Deproteinized bovine

Electronic supplementary material The online version of this article (https://doi.org/10.1007/s00784-019-03181-8) contains supplementary material, which is available to authorized users.

✉ Nikola Saulacic
nikola.saulacic@insel.ch

[1] Department of Cranio-Maxillofacial Surgery, Berne University Hospital Faculty of Medicine, University of Berne, Freiburgstrasse 10, 3010 Berne, Switzerland

[2] Geistlich Pharma AG, Bahnhofstrasse 40, 6110 Wolhusen, Switzerland

[3] Advanced Research Center, The Nippon Dental University School of Life Dentistry at Niigata, 1-8 Hamauracho, Chuo-ku, Niigata 951-8580, Japan

bone mineral is a widely applied xenograft. Yet, it shows a slower and more incomplete resorption when compared to autogenous grafts [5, 6]. Alloplastic biomaterials such as calcium phosphates have been developed as an alternative to the xenografts [7, 8]. Calcium phosphates, in particular, hydroxyapatite (HA), and tricalcium phosphate (TCP) have been in the focus of biomaterial research due to their composition resembling natural bone. The degradation level of TCPs, however, is of a much higher rate compared to that of HA. TCPs are further divided into alpha-tricalcium phosphates (α-TCP) and beta-tricalcium phosphates (β-TCP) with both having distinct degradation patterns [9]. An osteoconductive potential has been recognized for both TCPs scaffolds, but the fast degradation rate resulted in unsatisfactory bone formation [7, 10–12]. Given that none of the currently available monophasic TCP bone substitute materials maintain sufficient space, biphasic calcium phosphates (BCPs) have been developed mainly comprising β-TCP and HA [13–15]. The degradation profile of BCPs should be in balance with a faster degrading component (TCP) in order to enhance the ingrowth of new bone [7, 10]. The kinetics of the replacement of the BCP is considered to be too slow, even after lowering the content of HA [16–20]. The change of β-TCP in favor of α-TCP was due to its higher solubility [12, 21] and accordingly more rapid degradation providing space for new bone formation. Unexpectedly, BCPs composed of HA and α-TCP [20] demonstrated low degradability and remarkable space maintaining properties up to 1 year of healing [22]. In another study on a BCP with an α-TCP core, biomimetic HA coating was blended with 10% of porcine collagen to form a putty and for placement into fresh extraction sockets of dogs [23]. The biomaterial demonstrated high osteoconductive potential but did not undergo marked resorption during bone remodeling and remained as a stable scaffold up to 3 months of healing. Presumably, a potential beneficial effect of the HA/α-TCP on bone formation may be assessed in a more challenging defect model.

The present study was designed to evaluate the influence of the addition of collagen to the biomimetic HA-coated BCP in particulate form using an animal model with critical-size defects. The aim was to determine the impact of two BCPs on bone formation and graft resorption by means of micro-CT and histology.

Materials and methods

Materials

The HA/α-TCP composite materials were kindly provided by Geistlich Pharma AG (Wolhusen, Switzerland). Bilayered BCP (BBCP) with an α-TCP core was epitactically coated with a biomimetic nanocrystalline HA layer of a defined thickness. The sintered core material was obtained by mixing powders of calcium and phosphate donors in appropriate ratios and sintering the mixture at high temperature. The coating was obtained through the transition of the sintered TCP core material into biomimetic HA. The used BBCPs were composed of 12% HA and 88% α-TCP. The biomimetic HA coating of BBCP yielded a crystal size of 18 × 18 × 38 nm similar to that observed for natural bone mineral. The BBCP putty comprised of 90% (w/w) BBCP particles and 10% (w/w) porcine collagen (BBCP_C). The collagen component was produced from the commercially available non-cross-linked collagen I/III membrane with bilayer structure (Bio-Gide®, Geistlich Pharma AG, Wolhusen, Switzerland) which was dry milled and mixed with the BBCP particles. The size of particles embedded in the collagen matrix ranged from 0.7 to 2.0 mm (Suppl. Fig. 1). The BBCP material had a total porosity of 70–80% and the surface of all particles presented numerous macropores. Each bone substitute was separately packed for each defect and sterilized before surgery.

Animals

Eighteen adult female New Zealand white rabbits (3.0–4.0 kg) were used for the study. During the acclimatization period and throughout the experiment, the animals were housed in the Central Animal Care Facility at the University of Berne (temperature 19–21 °C, humidity 45% ± 10%, a light/dark cycle of 12:12 h). The animals were housed without excessive or disturbing noises and fed with a standard diet and water ad libitum. The study considered the NC3Rs, UK guidelines, and is reported according to the ARRIVE guidelines for preclinical in vivo studies. The study was submitted to and approved by the Committee for Animal Research, Canton of Berne, Switzerland (Nr: BE 89/17).

Anesthesia and surgery

The premedication of the animals was done with ketamine 65 mg/kg s.c (Narketan®, Vetoquinol AG, Berne, Switzerland), xylazine 4 mg/kg (Xylapan®, Vetoquinol AG, Berne, Switzerland), and buprenorphine 0.03 mg/kg (Temgesic®, Rechitt Benckiser, Wallisellen, Switzerland) in the neck area mixed in the same syringe. The animals were left undisturbed for 10 to 15 min to reach the appropriate depth of sedation. The eyes were lubricated (Bepanthen Augen- und Nasensalbe, Bayer Vital GmbH, Leverkusen, Germany) and pure oxygen administered by a facemask. The anesthesia was maintained with isoflurane (0–1%) (Forene, Abbvie AG, Baar, Switzerland) vaporized in pure oxygen through a Jackson Rees modified T-piece breathing system. Meloxicam 0.3 mg/kg s.c. (Metacam®, Boehringer Ingelheim, Ingelheim, Germany) and penicillin 150,000 IU/mL + benzathine penicillin 150,000 IU/mL s.c. (Duplocillin®, MSD Animal Health, Luzern, Switzerland) were administered prior to surgery and 0.01 mL/kg NaCl

0.9% 5 mL/kg/h (B. Braun Medical AG) throughout the procedure.

The surgical area was shaved and disinfected, and a local anesthesia was introduced with 0.5 mL of 1% lidocaine HCl (Lidocaïne, Bichsel, Interlaken, Switzerland). The skin was incised from the nasal bone to the mid-sagittal crest, and the periosteum was elevated to expose the parietal bone. Two 10-mm diameter bone defects were prepared with a trephine under copious irrigation with sterile saline. Maximal care was taken to avoid injury of the *dura mater*.

The following three treatment modalities were randomly allocated: (i) sham (empty), (ii) BBCP, and (iii) BBCP_C. The weight of the biomaterials was about 0.15 g per defect. Allocation of the applied treatment modalities was randomized according to the systematic random protocol (www.randomization.com). Prior to implantation, 600 μL of blood were collected from the auricular artery using a 22G iv. catheter (Vasofix® Safety, B. Braun Melsungen AG, Sempach, Switzerland). About 300 μL of the blood was mixed with each biomaterial. Another 300 μL was used for the negative control (sham). After implantation, the defects were covered with a non-cross-linked porcine collagen membrane (Geistlich Bio-Gide®, Geistlich Pharma AG, Wolhusen LU, Switzerland). The periosteum and skin were closed in two layers with interrupted sutures using 4–0 Vicryl® and 4–0 Monocryl® sutures (Ethicon, Somerville, NJ, USA), respectively, and the wound surfaces were sealed with a spray film dressing (OPSITE® SPRAY, Smith & Nephew, London, UK).

Following surgery, the rabbits were left to recover under infrared lights and administration of oxygen. For postoperative analgesia, buprenorphine 0.03 mg/kg s.c. every 8 h for 3 days and meloxicam 0.3 mg/kg once daily for 5 days were used. Monitoring included assessment of water and food consumption and pain at regular intervals (composite pain scale and grimace scale). Rescue analgesia was administered if necessary.

Euthanasia

One rabbit had to be euthanized because of neurological symptoms on the first day after surgery. Thus, 17 rabbits were sacrificed after healing periods of 3 weeks ($n = 9$) and 3 months ($n = 8$), respectively. Animals were premedicated with ketamine 65 mg/kg and xylazine 4 mg/kg s.c. in the neck area. Euthanasia was performed with an overdose of pentobarbital 120 mg/kg i.v. (Streuli Pharma AG, Uznach, Switzerland). Following sacrifice, the harvested specimens were analyzed by means of micro-CT and histologically.

Micro-CT analysis

Following harvesting, the treated sites were fixed in 10% neutral formalin for 7 days at room temperature then replaced in 70% ethanol at 4 °C, followed by PBS rinsing. The specimens were then subjected to micro-CT scans using a desktop cone-beam scanner (micro-CT 40, Scanco Medical AG, Brüttisellen, Switzerland). The X-ray source was set at 70 kV with 114 μA. An isotropic voxel size of 18 μm showed an image matrix of 2048 × 2048 pixels. The micro-CT images were then analyzed and reconstructed by using 3D structural analysis software (Amira, Visualization Sciences Group, Düsseldorf, Germany). The volume of interest (VOI) was selected corresponding to the dimensions of the defect sites, with a diameter of 10-mm full-thickness cylinders. The micro-CT data of the biomaterials and harvested bone were used as reference threshold values for the analyses of tested groups. Bone volume (BV, mm^3), bone density (BD, relative % to initial bone at the defect site), residual graft volume (RGV, mm^3), residual graft density (RGD, relative % to initial bone at the defect site), mineralized tissue volume (MTV, BV + RGV), and mineralized tissue density (MTD, relative % to initial bone at the defect site) were calculated after the segmentation.

Histomorphometry

The specimens were trimmed, dehydrated in ascending concentrations of ethanol, and embedded in methyl methacrylate without decalcification. The embedded tissue blocks were cut sagittally at the middle of the defects into approximately 800 μm thick ground sections using a slow-speed diamond saw (VC-50; LECO, St. Joseph, MI, USA). After mounting on acrylic glass slabs, the sections were ground and polished to a final thickness of 200 μm (Knuth Rotor-3; Struers, Ballerup, Denmark). The labeled bone was digitally photographed under a fluorescent microscope (Nikon Eclipse E800; Nikon, Tokyo, Japan). The sections were stained with toluidine blue combined with fuchsin. The images were photographed under a Wild Heerbrugg M400 ZOOM Makroskop for overviews and a light microscope (Nikon Eclipse E800) equipped with a digital imaging system (NIS Elements; Nikon) for the morphometric analysis. Morphometric analysis was performed by a graphic software (Photoshop CS6; Adobe, San Jose, CA, USA) using the corresponding 10-mm initial defect area as the region of interest (ROI). The parameters including horizontal defect closure (%), new bone area (NBA, relative % to total augmentation area), bone marrow area (BMA, relative % to total augmentation area), residual graft area (RGA, relative % to total augmentation area), mineralized tissue area (MTA, NBA + RGA), and connective tissue area (CTA, relative % to total augmentation area) were calculated.

Statistical analysis

For all the quantitative data, the means and all plots of values were represented. The statistical analysis was done by one-way analysis of variance (ANOVA) with Tukey test by a

statistical program (GraphPad Prism 7.0 software; GraphPad Software, Inc., La Jolla, CA, USA). The level of significance was set at $\alpha = 0.05$.

Results

By the time of sacrifice, there were no signs of wound dehiscence, exposure, inflammation, or infection at the surgical sites. However, two defects in two animals with 3 weeks healing period had to be excluded from the analysis due to the damage of the *dura mater*. A total of 32 defects ($n = 32$) were analyzed. A sample size per a given healing period consisted of five defects ($n = 5$) for sham and BBCP groups, respectively, and six defects ($n = 6$) for BBCP_C group.

Micro-CT analysis

At 3 weeks of healing, new bone ingrowth was observed at peripheral areas of the defect in all groups, infiltrated into the gaps between the granules (Fig. 1). The quantitative analysis showed no significant differences in the BV between any of the groups, while BBCP_C showed a significantly higher BD as compared with the negative control (Table 1). All granules displayed a homogenous density, while the number of granules was higher in the BBCP group compared to the BBCP_C group. The defects treated with BBCP_C were less filled as compared to BBCP, but MTV and MTD were not different between BBCP and BBCP_C.

At 3 months, new bone was seen also at the central area of the defects between the BBCP particles (good osteoconductive potential) and to a lesser extent in the BBCP_C group. The quantitative analysis showed no significant differences in the BV or BD between any of the groups (Table 2). Defects treated with BBCP appeared to have higher bone fill than with BBCP_C. However, significant differences in MTV and MTD were observed only when comparing with the sham-operated but not between the test groups.

When compared longitudinally from 3 weeks to 3 months, both BV and BD in all groups significantly increased (Fig. 2). Moreover, RGV decreased and RGD increased. Significant changes in MTV were observed for the sham-operated and the BBCP_C sites, while in MTD only for the sham-operated sites.

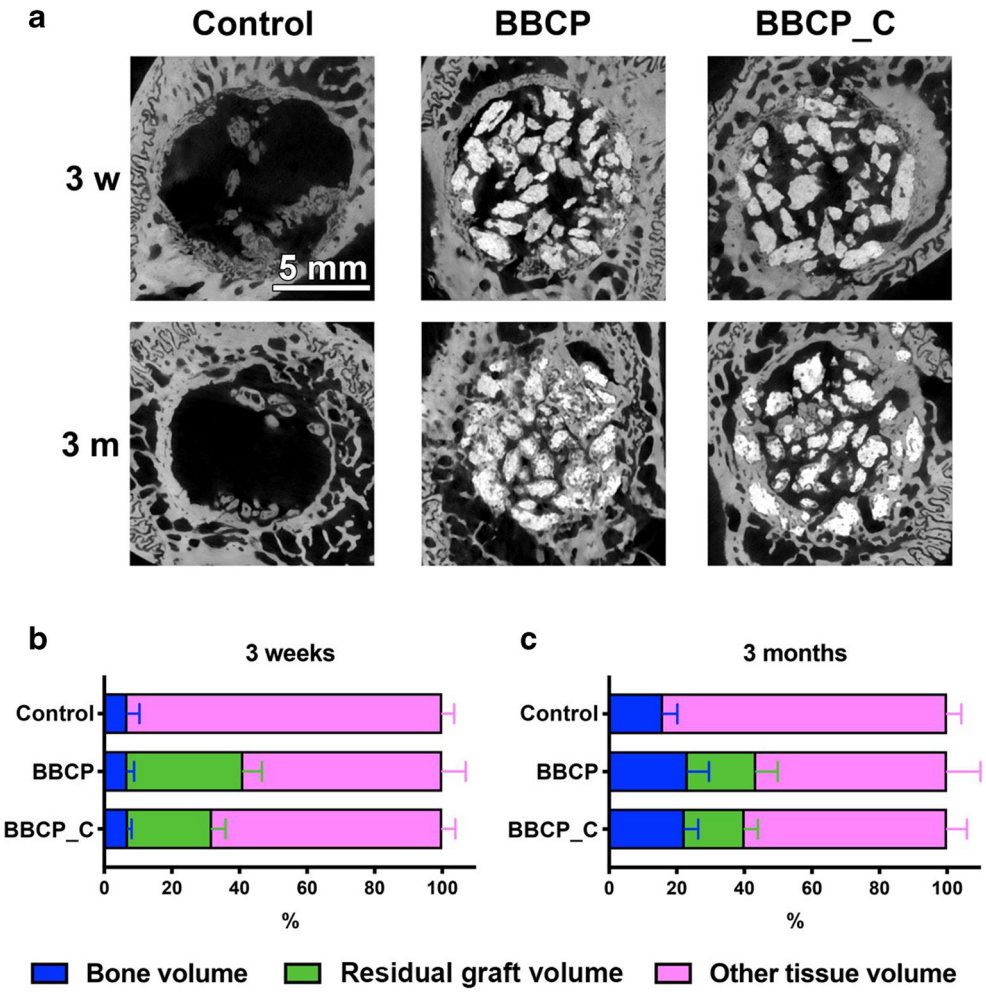

Fig. 1 (**A**) The micro-CT images of control (empty), BBCP, BBCP_C at 3 weeks, and 3 months post-surgery. Percentages of bone volume of material volume to total volume at 3 weeks (**B**) and 3 months (**C**). The graphs represent average values and SD

Table 1 Micro-CT measurements at 3 weeks post-surgery (mean ± SD). NS represents no significance between any groups

Micro-CT parameter	Experimental group			Statistics
	(1) Control	(2) BCP	(3) BCP-C	
Bone volume (mm^3)	13.27 ± 6.99	15.80 ± 4.77	16.58 ± 1.91	NS
Residual graft volume (mm3)		78.80 ± 12.97	58.66 ± 10.54	(2) vs (3)
Mineralized tissue volume (mm3)	13.27 ± 6.99	94.60 ± 16.70	75.23 ± 9.96	(1) vs (2) (3)
Bone density (relative % to initial bone)	81.50 ± 2.78	82.96 ± 1.96	85.20 ± 1.12	(1) vs (3)
Residual graft density (relative % to initial bone)		121.76 ± 4.13	122.49 ± 3.23	NS
Mineralized tissue density (relative % to initial bone)	81.50 ± 2.78	115.39 ± 3.97	114.17 ± 3.14	(1) vs (2) (3)

Histological observation

Ex vivo examination

After mixing with blood, all granules of both bone graft substitutes were surrounded with a corona of blood cells hardly infiltrated into the granules (Suppl. Fig. 2). White blood cells and erythrocytes were found within the collagen fibers of BBCP_C.

Descriptive histology

Generally, no signs of local inflammation or infections were observed in any of the samples (Fig. 3). Remnants of the collagen membrane were still observed at 3 weeks (Fig. 3a, c and e). In the peripheral areas of the defects, ingrowth of the newly formed woven bone was observed from the edges of the pristine bone (Fig. 3b, d and f). The granules of both biomaterials showed good contact with the new woven bone at the periphery of the defects and focally in the vicinity of the *dura mater*. However, newly formed bone was restricted to the surface of the particles and occasionally, to the large pores (Suppl. Figs. 3, 4). In the central areas of the defects, the granules of both groups were embedded in connective tissue. The connective tissue was cell poor and highly vascularized. Multinucleated giant cells (MNGC) were found surrounding the granules in both groups (Suppl. Fig. 5). The BBCP_C granules displayed less extent of osseointegration and higher number of MNGC on its surface.

At 3 months of healing, newly formed bone was observed in the central area of all groups (Fig. 3g, i and k). In most of the sections, the newly formed bone was adjacent to the *dura mater* rather than on the periosteal sides. New bone was observed throughout the whole defect in all BBCP samples and in 3 out of the 5 BBCP_C samples. The space between the periosteum and the *dura mater* in the central region was maintained in both test groups. No remnants of the collagen membranes could be identified at this time. New bone in the central region of BBCP and BBCP_C group was composed mainly of lamellar rather than woven bone. At the periphery mainly lamellar bone was found (Fig. 3j, l). Structures resembling bone forming units (osteons) were observed in bone surrounding granules, but also, they were perforating the granules (Suppl. Fig. 6). Nonintegrated granules were covered with a great number of MNGC and a fibrous capsule (Suppl. Fig. 7). An advanced differentiated, functional bone marrow was observed in all samples, mainly located at the defect borders.

Table 2 Micro-CT measurements at 3 months post-surgery (mean ± SD). NS represents no significance between any groups

Micro-CT parameter	Experimental group			Statistics
	(1) Control	(2) BCP	(3) BCP-C	
Bone volume (mm^3)	36.29 ± 7.74	54.71 ± 17.43	54.38 ± 9.73	NS
Residual graft volume (mm3)		46.41 ± 13.84	43.38 ± 10.73	NS
Mineralized tissue volume (mm3)	36.29 ± 7.74	100.78 ± 25.44	98.74 ± 17.46	(1) vs (2) (3)
Bone density (relative % to initial bone)	90.53 ± 2.57	92.39 ± 2.24	91.43 ± 3.06	NS
Residual graft density (relative % to initial bone)		139.04 ± 2.79	138.09 ± 1.70	NS
Mineralized tissue density (relative % to initial bone)	90.53 ± 2.57	113.55 ± 4.70	111.91 ± 4.02	(1) vs (2) (3)

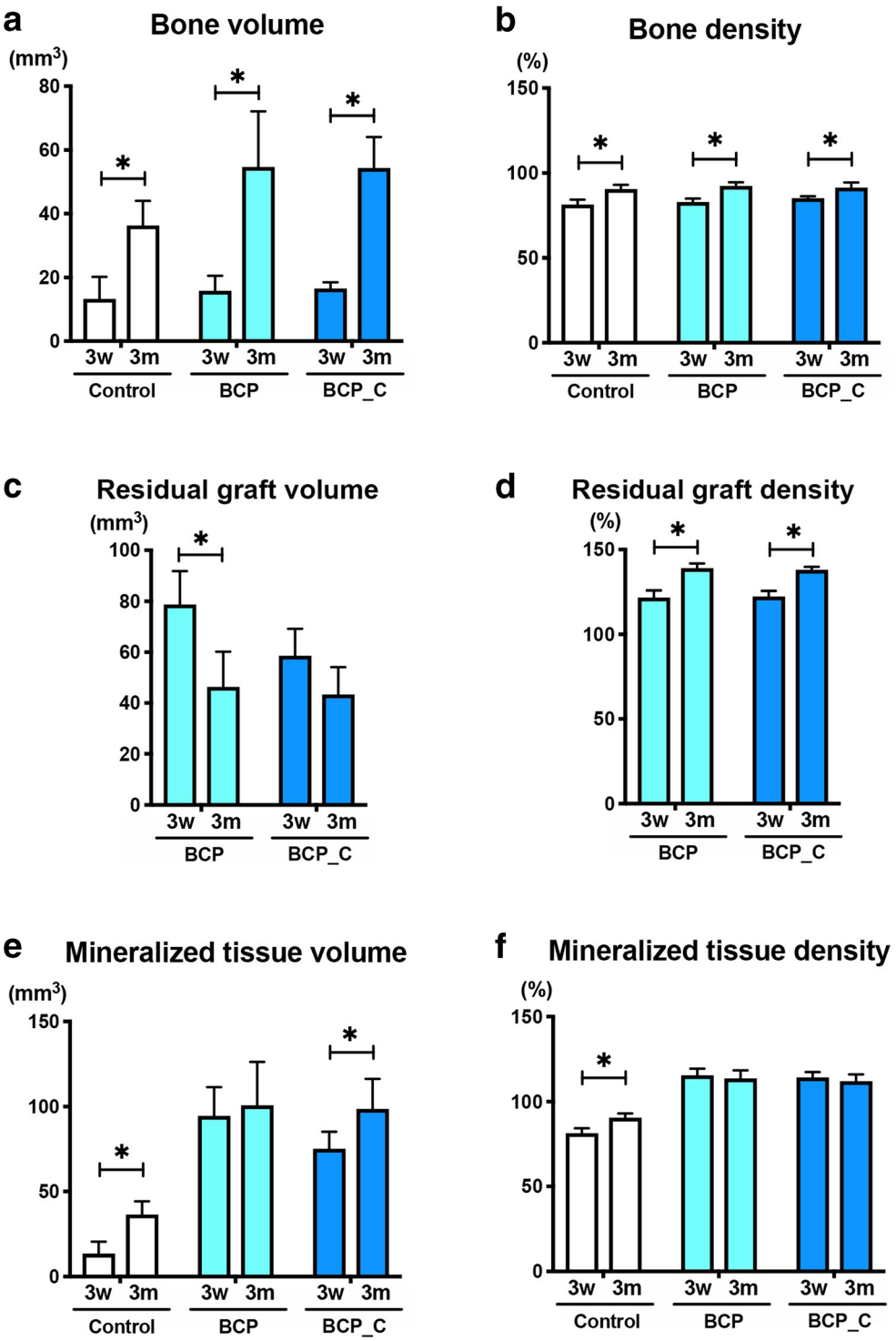

Fig. 2 The comparison of 3 weeks and 3 months for micro-CT results including (**A**) bone volume (mm^3), (**B**) bone density (relative % to initial bone density), (**C**) residual graft volume (mm^3), and (**D**) residual graft density (relative % to initial bone density), (**E**) mineralized tissue volume (mm^3; bone volume + material volume), and (**F**) mineralized tissue density (relative % to initial bone density). *denotes significant difference between 3 weeks and 3 months ($p < 0.05$)

Histomorphometry

The percentage of horizontal defect closure with new bone was not significantly different between the three groups at 3 weeks but between the two test groups and the sham-operated sites at 3 months (Tables 3, 4). Sham-operated sites demonstrated significantly more NBA than the two test groups after 3 weeks of healing (Fig.4; Table 3), whereas after 3 months, the values obtained were similar for all groups (Fig.4; Table 4). RGA was not different between the two test groups. Both biomaterials tested showed lower percentages of CTA and higher MTA when compared to the control group. The absolute values of the area parameter analyses (mm^2) are not

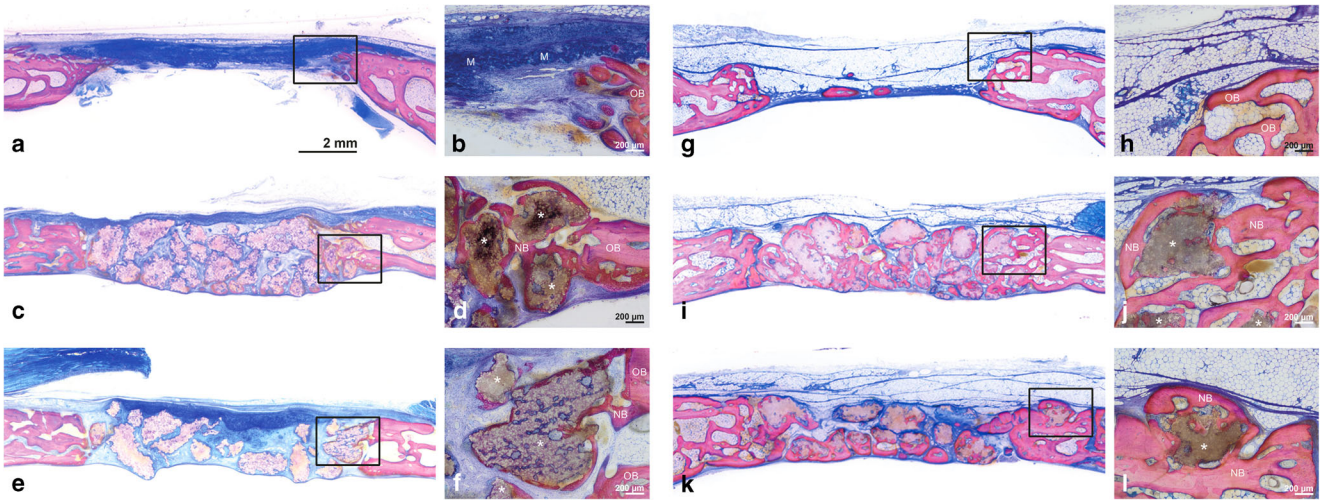

Fig. 3 Histological images of the center of the defect representing control (a, b, g, h), BBCP (c, d, i, j) and BBCP_C groups (e, f, k, l). (a–f) At 3 weeks of healing, new bone is observed at the peripheral areas of the defect. The outlined areas in (a, c, e) are magnified in (b, d, f). (b) The remnants of membranes (M) are detectable covering the defect and the old bone (OB). (d, f) Both groups of granules (*) are showing contact to the newly formed bone (NB). (g–l) At the 3 months of healing, new bone is seen in the central areas of the defect. The outlined areas in (g, i, k) are magnified in (h, j, l). (j, l) At the periphery of the defect, both types of granules (*) are integrated in a newly formed lamellar bone (NB) (toluidine blue and fuchsin staining)

shown, as the tendencies of the results were similar to those of the relative percentages.

When comparing the 3 weeks to the 3 months results, NBA significantly increased in all three groups (Fig. 5). The defect closure and BMA increased significantly only in the two test groups. In all three groups, CTA significantly decreased while MTA significantly increased.

Discussion

In the present study, the effects of two bone substitutes prototypes containing the same biomimetic HA/α-TCP composite material differed with regard to presence or absence of collagen was assessed on bone tissue formation and biomaterial resorption during healing of critical size defects in rabbits. Both types of BBCP were osteoconductive and yielded the same rate of bone formation. Collagen is thus confirmed as a carrier material for the BBCP granules, but it did not improve the osteogenic capacity in this particular defect.

Direct contact between the bone and the biomaterial at the margin of the defects during early healing was observed for both biomaterials, as already previously shown for HA/β-TCP [18]. Lindhe et al. [23] found higher NBA for a BCP with an α-TCP core and a biomimetic HA coating mixed with 10% collagen at 1 and 3 months of healing than in the present study. This difference may be explained by the use of intact extraction socket of that study as compared to the critical size defects used in the present study. Furthermore, BBCP_C showed greater space between the particles when compared to BBCP

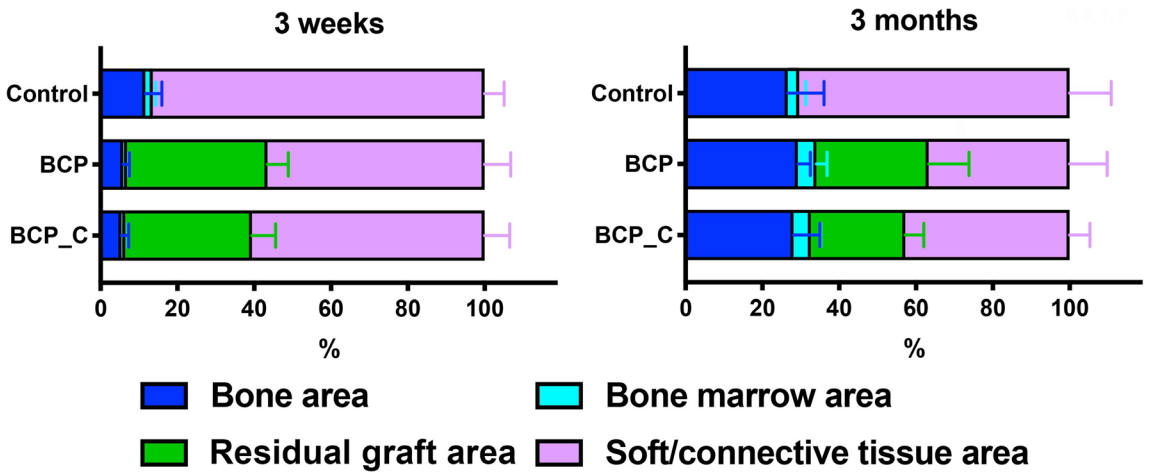

Fig. 4 Histomorphometrical data showing the percentage of each parameter at 3 weeks and 3 months of healing. The graph represents average and SD

Table 3 Histolomorphometry at 3 weeks post-surgery (mean ± SD). NS represents no significance between any groups

Micro-CT parameter	Experimental group			Statistics
	(1) Control	(2) BCP	(3) BCP-C	
Horizontal defect closure (%)	45.65 ± 28.17	43.29 ± 16.87	34.82 ± 13.55	NS
Bone area (%)	11.64 ± 4.33	5.92 ± 1.62	5.48 ± 1.83	(1) vs (2) (3)
Bone marrow area (%)	1.94 ± 0.80	0.98 ± 0.46	0.94 ± 0.74	NS
Residual graft area (%)		36.55 ± 5.43	33.00 ± 6.19	NS
Soft/connective tissue (%)	86.42 ± 5.10	56.56 ± 6.83	60.58 ± 6.51	(1) vs (2) (3)
Mineralized tissue area (%)	11.64 ± 4.33	42.46 ± 6.79	38.48 ± 6.15	(1) vs (2) (3)
Total augmentation area (mm^3)	13.28 ± 3.22	27.25 ± 3.51	24.65 ± 4.55	(1) vs (2) (3)

(Fig. 1a). Mixing of BBCP with collagen actually reduced the number of the granules potentially impairing the osteoconductivity. The presence of collagen was supposed to enhance the osteogenic response, as previously reported to exert the strong influence on ectopic bone formation [24]. Clearly, such an impact has not been observed in the present experimental set up. The same osteogenic potential for both materials was detected by micro-CT and morphometric analysis.

BBCP_C showed less RGV and RGA at both healing periods, but the significant difference was detected only for RGV at 3 weeks; it is possible that a statistical significance could be reached increasing the number of animals per group and healing period. As approximately the same amount of biomaterial was used for each defect, these differences may be related to the presence of collagen within BBCP_C. Efficient blood uptake by both prototypes was observed prior to biomaterial placement. Polymorphonuclear cells and monocytes/macrophages were the major cell types instantly in contact with the biomaterials after their application. Macrophages have been identified to play an essential role in resorption of biomaterials [25] and are key cells in biomaterial induced bone formation [26]. As the layers of MNGC surrounded the granules, a cell-dependent degradation of the biomaterial should be considered. The formation and presence of MNGC did not hinder bone formation. As such, a classical foreign body reaction may be excluded, the latter leading to isolation of biomaterials and consecutive clinical failure [27]. The role of MNGC in bone graft augmentation certainly needs further research.

New bone was either separated from the particles by a connective tissue layer or restricted to the surface of the particles. No difference was observed for the two tested groups. Consequently, the collagen component did not act as guiding structure for the enhancement of bone formation.

It is known that the pores are necessary for vessel ingrowth prior to bone formation [28]. The small diameter of the interconnected pore system in the two BBCPs apparently restricted cell/tissue uptake and bone formation to the surface of the granules. The presence of cell accessible pores might be decisive for the degradation/resorption of the biomaterial and formation of new bone. This aspect will be considered in future studies using biomaterials with different pore sizes.

Both biomaterials degraded from 3 weeks to 3 months of healing, showing rather similar behavior as the granular HA/β-TCP [19]. These in vivo data, however, are in contrast with the findings for a BCP material with an α-TCP core and a biomimetic HA coating mixed with 10% collagen in a putty form used in a previous study [23] or for HA/α-TCP in block form [20, 22]. It is possible that the macroporosity of the biomaterials was an important factor leading to the differences in degree of degradation/resorption [29, 30]. Both types of BBCPs provided sufficient space between the *dura mater*

Table 4 Histolomorphometry at 3 months post-surgery (mean ± SD). NS represents no significance between any groups

Micro-CT parameter	Experimental group			Statistics
	(1) Control	(2) BCP	(3) BCP-C	
Horizontal defect closure (%)	56.31 ± 21.08	99.60 ± 0.49	95.26 ± 7.21	(1) vs (2) (3)
Bone area (%)	26.59 ± 9.51	29.27 ± 3.24	28.12 ± 6.90	NS
Bone marrow area (%)	3.00 ± 1.74	4.82 ± 2.78	4.47 ± 2.63	NS
Residual graft area (%)		29.23 ± 10.49	24.62 ± 4.83	NS
Soft/connective tissue (%)	70.41 ± 10.84	36.69 ± 9.75	42.79 ± 5.29	(1) vs (2) (3)
Mineralized tissue area (%)	26.59 ± 9.51	58.49 ± 9.85	52.74 ± 2.84	(1) vs (2) (3)
Total augmentation area (mm^3)	11.62 ± 2.34	22.35 ± 4.93	24.42 ± 4.04	(1) vs (2) (3)

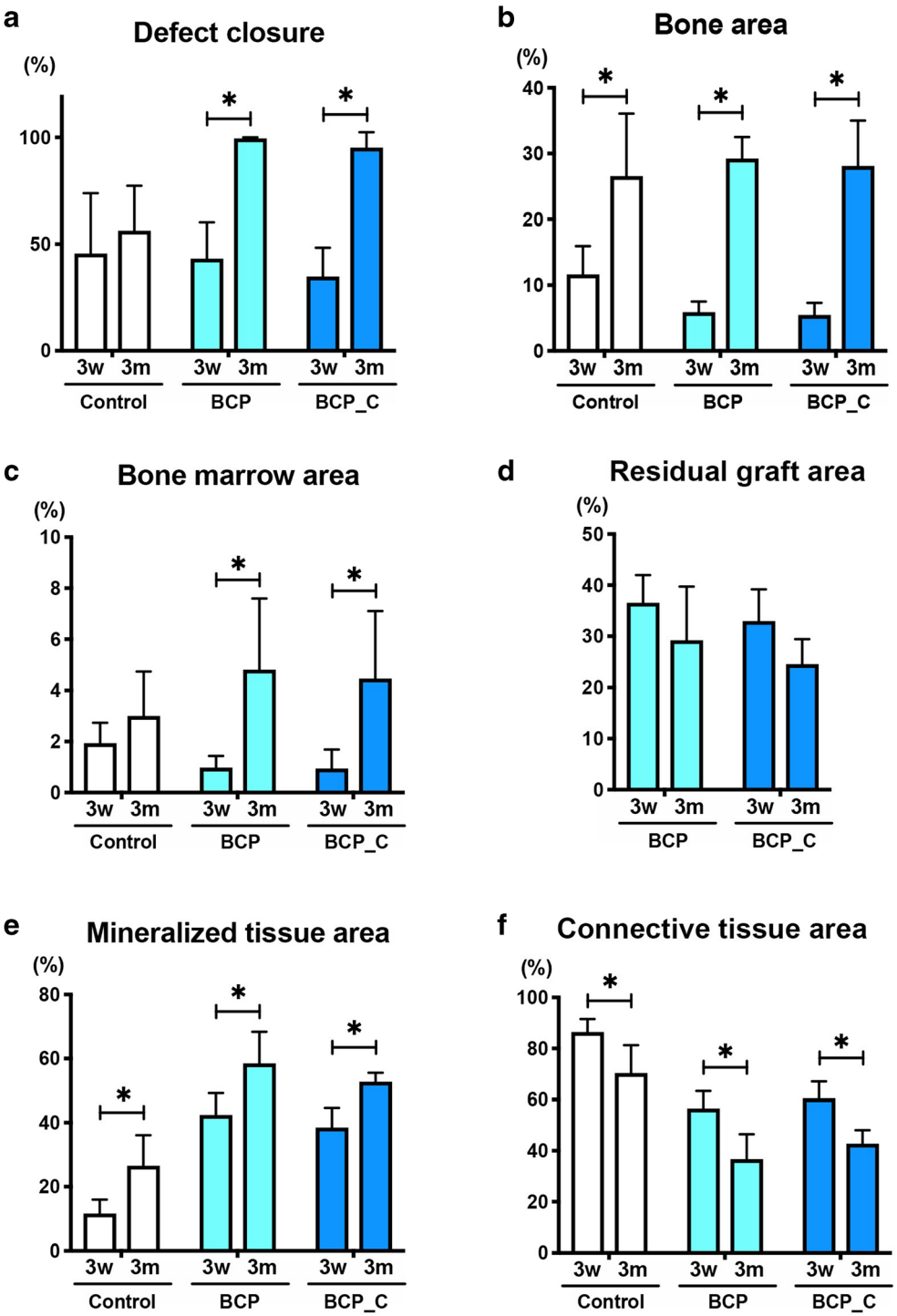

Fig. 5 The comparison of histomorphometric results between 3 weeks and 3 months; (**A**) horizontal defect closure (%), (**B**) new bone area (% to total augmentation area), (**C**) bone marrow area (% to total augmentation area), (**D**) residual graft area (% to total augmentation area), (**E**) mineralized tissue area (bone area + material area; % to total augmentation area), and (**F**) connective tissue area (% to total augmentation area). *denotes significant difference between 3 weeks and 3 months ($p < 0.05$)

and the periosteum for bone formation. Mature bone marrow including the presence of well-developed osteons and interstitial lamellae in particular in the periphery of the defects indicated an advanced stage of bone modeling and remodeling. The space maintaining capacity of the biomaterials tested, controlled by their degradation and formation of new bone, should be further assessed in a study with a longer follow-up period.

Conclusions

Within the limits of this study, two biomaterials used showed good biocompatibility and osteoconduction. Both biomaterials induced similar amounts of bone formation, leading to the healing of a critical size defects. The addition of collagen may successfully be used as a carrier material for BBCP but does not have a significant impact on the outcome.

Acknowledgments The authors wish to thank the staff at the ESI, Surgical Unit, DBMR, University of Bern, Switzerland, for excellent handling of the animals, Mr. Mark Siegrist for his assistance during μCT evaluation and Ms. Inga Grigaitiene for the histological preparation. The synthetic bone substitutes were kindly provided by Geistlich Pharma AG (Wolhusen, Switzerland).

Funding information The study was supported by the Department of Cranio-Maxillofacial Surgery, Faculty of Medicine, University of Berne, Switzerland.

Compliance with ethical standards

Conflict of interest All authors declare that they have no conflict of interest.

Ethical approval The study protocol was approved from the Committee for Animal Research, Canton of Berne, Switzerland (Nr: BE 89/17).

Informed consent For this type of study, formal consent is not required.

References

1. Miron RJ, Hedbom E, Saulacic N, Zhang Y, Sculean A, Bosshardt DD, Buser D (2011) Osteogenic potential of autogenous bone grafts harvested with four different surgical techniques. J Dent Res 90: 1428–1433
2. Nkenke E, Stelzle F (2009) Clinical outcomes of sinus floor augmentation for implant placement using autogenous bone or bone substitutes: a systematic review. Clin Oral Implants Res 20(Suppl 4):124–133
3. Wang RE, Lang NP (2012) Ridge preservation after tooth extraction. Clin Oral Implants Res 23(Suppl 6):147–156
4. Williams RJ, Gamradt SC (2008) Articular cartilage repair using a resorbable matrix scaffold. Instr Course Lect 57:563–571
5. Kolerman R, Samorodnitzky-Naveh GR, Barnea E, Tal H (2012) Histomorphometric analysis of newly formed bone after bilateral maxillary sinus augmentation using two different osteoconductive materials and internal collagen membrane. Int J Periodontics Restorative Dent 32:e21–e28
6. Mordenfeld A, Hallman M, Johansson CB, Albrektsson T (2010) Histological and histomorphometrical analyses of biopsies harvested 11 years after maxillary sinus floor augmentation with deproteinized bovine and autogenous bone. Clin Oral Implants Res 21:961–970
7. Hwang JW, Park JS, Lee JS, Jung UW, Kim CS, Cho KS, Lee YK, Choi SH (2012) Comparative evaluation of three calcium phosphate synthetic block bone graft materials for bone regeneration in rabbit calvaria. J biomed mater res. B Appl Biomat 100:2044–2052
8. Torres J, Tamimi F, Alkhraisat MH, Prados-Frutos JC, Rastikerdar E, Gbureck U, Barralet JE, Lopez-Cabarcos E (2011) Vertical bone augmentation with 3D-synthetic monetite blocks in the rabbit calvaria. J Clin Periodontol 38:1147–1153
9. Rojbani H, Nyan M, Ohya K, Kasugai S (2011) Evaluation of the osteoconductivity of alpha-tricalcium phosphate, beta-tricalcium phosphate, and hydroxyapatite combined with or without simvastatin in rat calvarial defect. J Biomed Mater Res A 98:488–498
10. Hirota M, Matsui Y, Mizuki N, Kishi T, Watanuki K, Ozawa T, Fukui T, Shoji S, Adachi M, Monden Y, Iwai T, Tohnai I (2009) Combination with allogenic bone reduces early absorption of beta-tricalcium phosphate (beta-TCP) and enhances the role as a bone regeneration scaffold. Experimental animal study in rat mandibular bone defects. Dent Mater J 28:153–161
11. Habibovic P, Yuan H, van der Valk CM, Meijer G, van Blitterswijk CA, de Groot K (2005) 3D microenvironment as essential element for osteoinduction by biomaterials. Biomaterials 26:3565–3575
12. Carrodeguas RG, De Aza S (2011) Alpha-tricalcium phosphate: synthesis, properties and biomedical applications. Acta Biomater 7:3536–3546
13. Daculsi G, Laboux O, Malard O, Weiss P (2003) Current state of the art of biphasic calcium phosphate bioceramics. J Mater Sci Mater Med 14:195–200
14. Nery EB, LeGeros RZ, Lynch KL, Lee K (1992) Tissue response to biphasic calcium phosphate ceramic with different ratios of HA/beta TCP in periodontal osseous defects. J Periodontol 63:729–735
15. Bouler JM, Pilet P, Gauthier O, Verron E (2017) Biphasic calcium phosphate ceramics for bone reconstruction: a review of biological response. Acta Biomater 53:1–12
16. Helder MN, van Esterik FAS, Kwehandjaja MD, Ten Bruggenkate CM, Klein-Nulend J, Schulten E (2018) Evaluation of a new biphasic calcium phosphate for maxillary sinus floor elevation: micro-CT and histomorphometrical analyses. Clin Oral Implants Res 29:488–498
17. Jensen SS, Bornstein MM, Dard M, Bosshardt DD, Buser D (2009) Comparative study of biphasic calcium phosphates with different HA/TCP ratios in mandibular bone defects A long-term histomorphometric study in minipigs. J Biomed Mater Res B App Biomater 90:171–181
18. Yang C, Unursaikhan O, Lee JS, Jung UW, Kim CS, Choi SH (2014) Osteoconductivity and biodegradation of synthetic bone substitutes with different tricalcium phosphate contents in rabbits. J Biomed Mater Res B App Biomater 102:80–88
19. Yip I, Ma L, Mattheos N, Dard M, Lang NP (2015) Defect healing with various bone substitutes. Clin Oral Implants Res 26:606–614
20. Carrel JP, Wiskott A, Moussa M, Rieder P, Scherrer S, Durual S (2016) A 3D printed TCP/HA structure as a new osteoconductive scaffold for vertical bone augmentation. Clin Oral Implants Res 27:55–62
21. Bohner M (2000) Calcium orthophosphates in medicine: from ceramics to calcium phosphate cements. Injury 31(Suppl 4):37–47
22. Sawada K, Nakahara K, Haga-Tsujimura M, Iizuka T, Fujioka-Kobayashi M, Igarashi K, Saulacic N (2018) Comparison of three block bone substitutes for bone regeneration: long-term observation in the beagle dog. Odontology 106:398–407
23. Lindhe J, Araujo MG, Bufler M, Liljenberg B (2013) Biphasic alloplastic graft used to preserve the dimension of the edentulous ridge: an experimental study in the dog. Clin Oral Implants Res 24: 1158–1163
24. Wagner-Ecker M, Voltz P, Egermann M, Richter W (2013) The collagen component of biological bone graft substitutes promotes ectopic bone formation by human mesenchymal stem cells. Acta Biomater 9:7298–7307
25. Sheikh Z, Brooks PJ, Barzilay O, Fine N, Glogauer M (2015) Macrophages, foreign body giant cells and their response to implantable biomaterials. Materials 8:5671–5701
26. Miron RJ, Bosshardt DD (2016) OsteoMacs: key players around bone biomaterials. Biomaterials 82:1–19
27. Anderson JM, Rodriguez A, Chang DT (2008) Foreign body reaction to biomaterials. Semin Immunol 20:86–100
28. Klenke FM, Liu Y, Yuan H, Hunziker EB, Siebenrock KA, Hofstetter W (2008) Impact of pore size on the vascularization and osseointegration of ceramic bone substitutes in vivo. J Biomed Mater Res A 85:777–786
29. Habibovic P, Kruyt MC, Juhl MV, Clyens S, Martinetti R, Dolcini L, Theilgaard N, van Blitterswijk CA (2008) Comparative in vivo

study of six hydroxyapatite-based bone graft substitutes. J Orthop Res 26:1363–1370

30. Park JW, Kim ES, Jang JH, Suh JY, Park KB, Hanawa T (2010) Healing of rabbit calvarial bone defects using biphasic calcium phosphate ceramics made of submicron-sized grains with a hierarchical pore structure. Clin Oral Implants Res 21: 268–276